IEEE Access
Multidisciplinary | Rapid Review | Open Access Journal

Received 1 April 2024, accepted 18 April 2024, date of publication 22 April 2024, date of current version 30 April 2024.

Digital Object Identifier 10.1109/ACCESS.2024.3392429

RESEARCH ARTICLE

Dynamic Quantum Federated Learning for Satellite-Ground Integrated Systems Using Slimmable Quantum Neural Networks

SOOHYUN PARK[1], SOYI JUNG[2], (Member, IEEE), AND JOONGHEON KIM[3], (Senior Member, IEEE)

[1]Division of Computer Science, Sookmyung Women's University, Seoul 04310, Republic of Korea
[2]Department of Electrical and Computer Engineering, Ajou University, Suwon 16499, Republic of Korea
[3]Department of Electrical and Computer Engineering, Korea University, Seoul 02841, Republic of Korea

Corresponding authors: Soyi Jung (sjung@ajou.ac.kr) and Joongheon Kim (joongheon@korea.ac.kr)

This work was supported by the Institute of Information and Communications Technology Planning and Evaluation (IITP) grant funded by Korean Government the Ministry of Science and Information and Communications Technology (MSIT), Information and Communications Technology (Development of 3D Spatial Satellite Communications Technology) under Grant 2021-0-00847.

ABSTRACT Recent advances in low Earth orbit (LEO) satellites have made it possible to achieve zero blind spots on Earth. Considering the give locations of these devices, this makes satellite-ground links between quantum devices a practical possibility. This paper proposes the first quantum federated learning (QFL) application in satellite-ground communication. To improve communication and computing performance, this paper adopts slimmable quantum federated learning (SQFL) and slimmable quantum neural networks (sQNN), which allow for two different configurations in quantum neural networks: the angle and pole configurations. This paper also employs superposition coding and successive decoding to increase communication opportunities. Through extensive experiments, the proposed satellite-ground SQFL framework performs well and is both computationally and communicationally efficient compared to classical federated learning and QFL.

INDEX TERMS Satellite-ground communication, quantum machine learning, quantum computing, federated learning.

I. INTRODUCTION

The global satellite communication market is expected to reach 45.3 billion dollars by 2027, with a compound annual growth rate of 8.1% from 2020 to 2027 [1]. This growth is driven by increasing demand for satellite-based broadband services and the adoption of advanced satellite technologies, such as high-throughput and low Earth orbit (LEO) satellites [2], [3], [4], [5], [6], [7]. LEO satellites have been used to provide communication networks in remote, transnational, or difficult-to-access areas. By utilizing LEO satellites, the local devices can easily access the resources of the satellites regardless of their locations [8]. Due to the aforementioned reasons, federated learning (FL) with different sites using LEO satellites has also been suggested as one of major potential applications [9], [10], [11], [12].

Quantum deep learning (QDL) devices are deployed in some locations because they are still a relatively new technology and only a limited number of them exist. They are often used for research purposes, and researchers from different institutions may need to access them for their work. By locating quantum computers in different areas, researchers from different institutions can use them easily for their research [13]. Utilizing LEO satellites in

The associate editor coordinating the review of this manuscript and approving it for publication was Jie Gao.

a federation of local quantum computers can benefit communication efficiency and computing power. In particular, the use of the movement range of orbiting LEO satellites could significantly reduce the fixed costs associated with transceiving trainable parameters through wired backhaul connections [14], [15].

Therefore, this paper considers leveraging quantum computers and satellite-ground communications in quantum federated learning (QFL) because of the potential benefits of communication efficiency and computing power that these technologies offer. Quantum computers have the ability to perform calculations more efficiently than classical computers, and quantum communication has the potential to be expanded [16], [17], [18]. In addition, this approach allows for the use of local resources. Quantum bits (qubits), the basic units of computation in a quantum computer, can be put into a superposition state and manipulated using quantum gates and measurement to perform certain tasks more efficiently [19], [20], [21]. As the number of qubits increases, it allows a larger quantum state space, known as superpositioned Hilbert space, which can potentially lead to quantum supremacy. One approach to taking advantage of the full potential of this state space is to use both a parameterized quantum circuit (PQC), known as the *angle* domain and a trainable measurement, known as the *pole* domain [22], [23]. The approach, known as slimmable quantum federated learning (SQFL [24], [25]), is used in our proposed framework. In this framework, local devices sequentially train their angle and pole parameters using their own data, and then send their encoded angle and pole parameters to the server using superposition coding (SC) during aggregation rounds. The server then decodes these messages using successive decoding (SD), which improves communication efficiency and performance compared to other quantum federated learning methods [26], [27], [28]. In addition, by utilizing slimmable neural networks in each local devices over quantum domain, the individual neural networks adpatively control their widths in order to deal with dynamic channel conditions. This nature of dynamic control is one of major differences from other QFL algorithms in [29], [30].

This paper presents a new approach to QFL that utilizes satellite-ground communications, the first QFL application to satellite-ground communications. Our method, based on SQFL, aims to take advantage of the benefits of quantum computing and improve communication opportunities compared to classical computing methods via SC and SD. The reason why the dynamic control nature in our proposed SQFL is essential for satellite-ground communications is that the satellite-based communications should be resilient in time-varying dynamic environments due to large propagation delays. In satellite communications, due to the long-distance between grounds and satellites, large propagation delays exist which is harmful for stabilized and robust communications. Therefore, dynamic control should be taken account in order to adapt the time-varying dynamic situations.

II. PRELIMINARIES

A. NOTATION AND MATHEMATICAL SETUP

This paper adopts the notation,

$$\Phi \triangleq [\boldsymbol{\phi}_1, \cdots, \boldsymbol{\phi}_n, \cdots, \boldsymbol{\phi}_N], \tag{1}$$

in order to represent the trainable parameters of the PQCs, *i.e.*, angle parameters. In addition,

$$\Theta \triangleq [\boldsymbol{\theta}_1, \cdots, \boldsymbol{\theta}_n, \cdots, \boldsymbol{\theta}_N] \tag{2}$$

denotes the trainable measurement parameters, *i.e.*, local pole parameters. The terms $\boldsymbol{\phi}_0$ and $\boldsymbol{\theta}_0$ denote the global angle parameters and pole parameters, respectively. A mini-batch from the local devices is defined as

$$\zeta_n \triangleq (\mathbf{X}_n, \mathbf{y}_n) \subset \mathbf{Z}_n, \tag{3}$$

where $(\mathbf{X}_n, \mathbf{y}_n)$ are the input data and corresponding labels, and $\mathbf{Z}_n$ is the full dataset of the local device n. The labels, *i.e.*,

$$\mathbf{y}_n \triangleq \{y_n^l\}_{l=1}^{|\mathbf{y}_n|} \tag{4}$$

are one-hot vectors with an 1 in the position corresponding to the true label and zeros in all other positions. This paper adopts Dirac notation to represent quantum states and operations, and the operators $(\cdot)^\dagger$ and $\otimes$ represent the complex conjugate transpose and tensor product, respectively.

B. QUANTUM OPERATIONS IN QNN

Fig. 1 represents a quantum neural network (QNN).[1] The architectures of QNN and our proposed sQNN consist of state encoder, PQC layer, and measurement, as illustrated in Fig. 1 and Fig. 2, respectively. Firstly, the state encoder is for (i) converting real-number domain information/data into quantum (3D Hilbert space) domain and (ii) angle encoding. This paper considers a system with Q qubits for QNN [31]. The basic quantum state is defined as

$$|\psi_0\rangle \triangleq |0\rangle^{\otimes Q}, \tag{5}$$

and classical data $\mathbf{X}$ is encoded into a quantum state $|\psi\rangle$ using a quantum state encoder $U_{enc}(\cdot)$, such that

$$|\psi\rangle = U_{enc}(\mathbf{X}) \cdot |\psi_0\rangle. \tag{6}$$

The Q qubit quantum state can also be expressed as follows,

$$|\psi\rangle = \sum_{n=0}^{2^Q-1} \alpha_n |n\rangle, \tag{7}$$

where α_n and $|n\rangle$ are the probability amplitudes and the n-th basis in the Hilbert space, respectively. The probability amplitudes α_n are complex numbers that satisfy the normalization

[1] All rotation gates (*e.g.*, RX and RY) and controlled gates in state encoder and PQC are expressed with unitary operations.

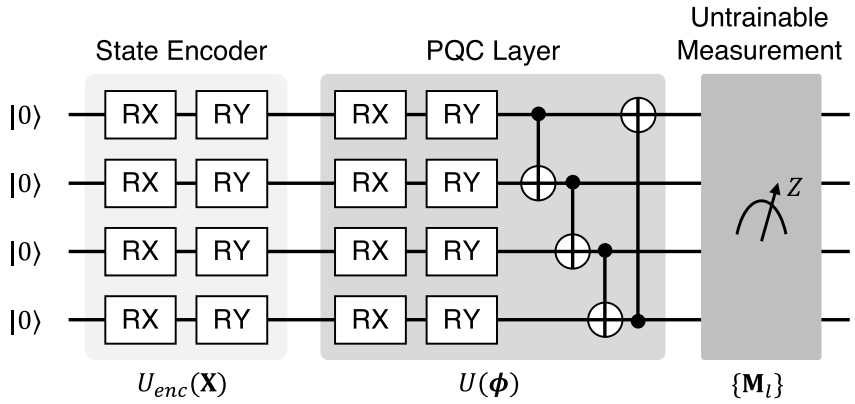

FIGURE 1. The architecture of QNN.

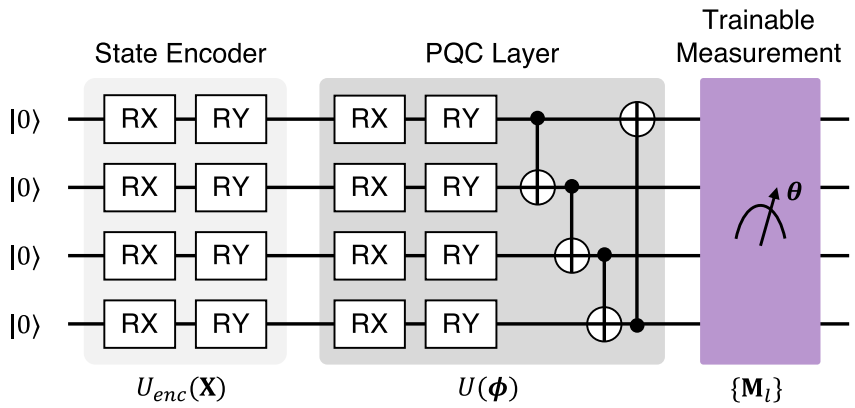

FIGURE 2. The architecture of sQNN.

condition, *i.e.*,

$$\sum_{n=1}^{2^Q} |\alpha_n|^2 = 1, \tag{8}$$

given that the Hilbert space is defined as $\mathscr{H}^{\otimes Q} \equiv \mathbb{C}^{2^Q}$. The quantum state $|\psi\rangle$ is then processed by a parameterized quantum circuit $U(\boldsymbol{\phi})$, such that

$$|\psi\rangle \leftarrow U(\boldsymbol{\phi}) \cdot |\psi\rangle. \tag{9}$$

Finally, the output is obtained by projecting the quantum state onto projection matrices $\mathbf{M}_l \in \{\mathbf{M}_l\}_{l=1}^{Q}$, one for each qubit l. The l-th projection matrix is defined as

$$\mathbf{M}_l \triangleq \mathbf{I}^{\otimes l-1} \otimes \mathbf{P}_Z \otimes \mathbf{I}^{\otimes Q-l}, \tag{10}$$

where $\mathbf{I}$ is the 2×2 identity matrix, and $\mathbf{P}_Z$ is Pauli-Z matrix, *i.e.*, $\mathbf{P}_Z \triangleq diag(1, -1)$. The expectation value of the projection $\mathbf{M}_l$ is denoted as $O_l \in \mathbb{R}[-1, 1]$, and can be calculated as

$$\langle O_l \rangle = \langle \psi | \mathbf{M}_l | \psi \rangle. \tag{11}$$

The expectation values of the projections are then used with the softmax function and a temperature parameter $\beta \in \mathbb{R}$ to make predictions for class l as,

$$\Pr(y = l) = \frac{\exp(\beta \langle O_l \rangle)}{\sum_{l'=1}^{q} \exp(\beta \langle O_{l'} \rangle)}, \tag{12}$$

where q denotes the number of classes.

As presented in [32], QNN-based learning models are advantageous comparing to conventional neural networks. First of all, it can achieve fast convergence by significantly reduce the number of iterations during loss function minimization. Moreover, it is possible to output dimension reduction into a logarithmic-scale by enhancing measurement, as discussed in [33]. Lastly, fewer parameter utilization for neural network models can be realized which is essentially beneficial in small-scale communication/memory-limited cube-satellite systems [34]. More detailed discussions for quantum algorithms design and implementation in modern noisy intermediate-scale quantum (NISQ) era are presented in [35], [36], and [37].

C. QUANTUM OPERATIONS IN SQNN

According to [38], QNN trains its feature map (*i.e.*, *angle domain*) by adjusting the PQC parameters. The QNN output is given by (10)-(11), which means that the measured qubit

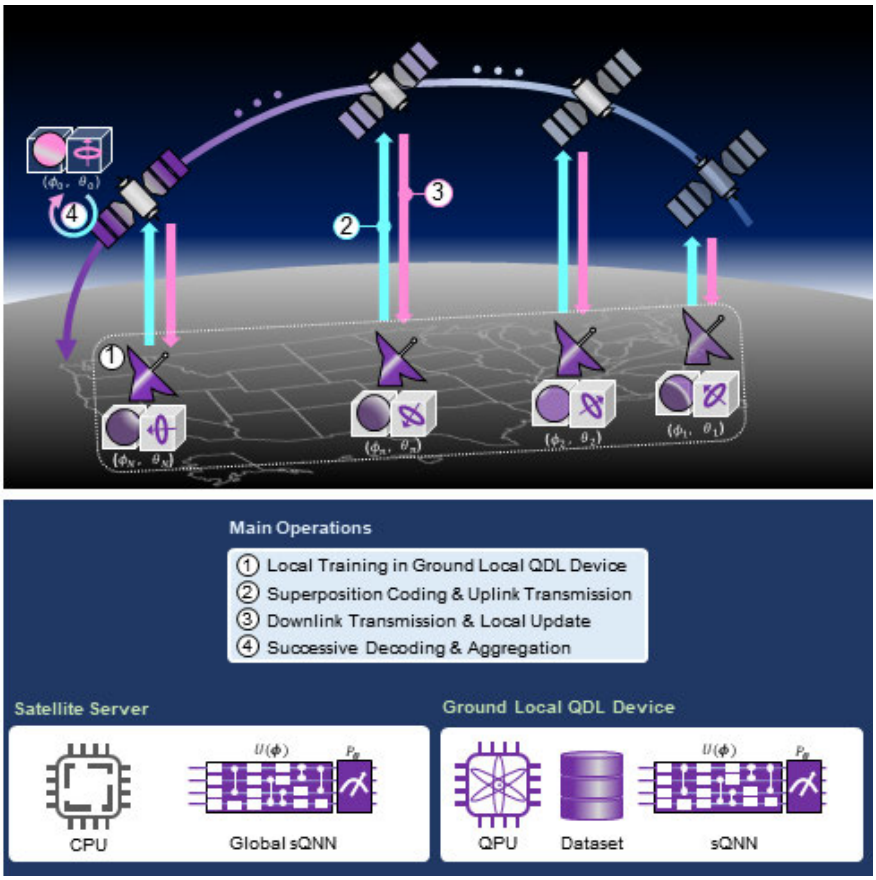

FIGURE 3. The illustration of satellite-ground SQFL framework. It consists of three processes: (1) local training and uplink transmission, (2) global model aggregation with successive decoding, (3) downlink transmission and update.

states are projected onto a hyperplane orthogonal to z-axis. (Schuld et al., 2022) demonstrates that hyperplane training (*i.e.*, *pole domain*) with a fixed feature map is possible [39]. Furthermore, the concept of slimmable neural networks is utilized for QNN [22], [24]. Fig. 2 represents the structure of sQNN. As shown in the figure, sQNN consists of two sub-networks: *i)* the trainable parameters of PQC and *ii)* the trainable measurement parameters (*i.e.*, pole parameters). The process of sQNN is exactly the same as the process of Sec. II-B except (10). The only difference is that $\mathbf{P}_Z$ in (10) is replaced to $\mathbf{P}_{\boldsymbol{\theta}}$ which is parameterized with $\boldsymbol{\theta}$ and acts as the projection operator for the sQNN. Based on this difference, our proposed sQNN can conduct the parameter training in measurement; where conventional QNN cannot do that. According to the trainability in measurement which is called *Pole-Training*, more flexibility can be reserved. When sQNNs are trained in distributed learning settings, the feature map is adjusted in the direction of having more generalized features, and the poles are fine-tuned to each local task [22]. In SQFL [24], the sequential local training of sQNN is proposed where pole parameters are first trained and then the angle parameters are trained next. This pole-to-angle training method shows the least performance degradation when local parameters are not successfully aggregated.

III. SLIMMABLE QUANTUM FEDERATED LEARNING IN LEO SATELLITE-GROUND COMMUNICATIONS

A. SYSTEM OVERVIEW

Fig. 3 represents our referencing satellite-ground SQFL framework. This paper considers a scenario with N local QDL devices tasked with performing classification. This paper adopts the channel model from [40], assuming that both satellite and ground QDL devices have a single antenna. We only consider uplink communications, in which each device sends two messages corresponding to two different width configurations. The bandwidth is equally divided among the devices, so inter-user interference is negligible. Notwithstanding, we still consider the inter-message interference due to superposition coding, which will be elaborated in Sec. III-C and III-D. This interference is treated as noise, and the Shannon capacity formula with a Gaussian codebook is used to analyze the communication performance [11].

B. POLE-TO-ANGLE LOCAL TRAINING

We describe pole-to-angle local training. The *pole* and *angle* parameters are denoted as $\boldsymbol{\phi}_n$ and $\boldsymbol{\theta}_n$, respectively, where the number of trainable parameters is 2 for $\boldsymbol{\phi}_n$ and D for $\boldsymbol{\theta}_n$. Since the number of parameters in $\boldsymbol{\phi}_n$ is smaller than $\boldsymbol{\theta}_n$, the pole,

Algorithm 1 Local Training in QDL Devices

Initialization. local-QNN parameters, $\boldsymbol{\phi}, \boldsymbol{\theta}$ **for** $t = \{1, 2, \ldots, T_{Local}\}$ **do**
  for $(\mathbf{X}, y) \in \mathbf{Z}$ **do**
    $\hat{y} \leftarrow \mathbf{sQNN}(\mathbf{X}; \boldsymbol{\phi}, \boldsymbol{\theta})$ // $\hat{y}$: logits
    Calculate loss, $\mathscr{L}(\boldsymbol{\phi}, \boldsymbol{\theta}, (\mathbf{X}, y))$
    Update pole, $\boldsymbol{\theta} \leftarrow \boldsymbol{\theta} - \eta_t \nabla_{\boldsymbol{\theta}} \mathscr{L}(\boldsymbol{\phi}, \boldsymbol{\theta}, (\mathbf{X}, y))$
$\tilde{\boldsymbol{\theta}} \leftarrow \boldsymbol{\theta}$ **for** $t = \{1, 2, \ldots, T_{Local}\}$ **do**
  for $(\mathbf{X}, y) \in \mathbf{Z}$ **do**
    $\hat{y} \leftarrow \mathbf{sQNN}(\mathbf{X}; \boldsymbol{\phi}, \tilde{\boldsymbol{\theta}})$
    Calculate loss, $\mathscr{L}(\boldsymbol{\phi}, \tilde{\boldsymbol{\theta}}, (\mathbf{X}, y))$
    Update angle, $\boldsymbol{\phi} \leftarrow \boldsymbol{\phi} - \eta_t \nabla_{\boldsymbol{\phi}} \mathscr{L}(\boldsymbol{\phi}, \tilde{\boldsymbol{\theta}}, (\mathbf{X}, y))$
$\tilde{\boldsymbol{\phi}} \leftarrow \boldsymbol{\phi}$

which is trained first, is expected to converge faster. Then, the angle is trained next and the angle domain shows more invariant robustness to covariate shift because the number of angle parameters is $\frac{D}{2}$x larger than pole parameters [41]. This paper conjectures that pole-to-angle local training will benefit the FL regime in which covariate shift exists due to data distribution. Algorithm 1 represents the local training in QDL devices. Each device trains pole parameters $\boldsymbol{\theta}$ for L iterations with mini-batch ζ_n sampled from the device's local dataset $\mathbf{Z}_n$. Then, the device trains angle parameters $\boldsymbol{\phi}$. For the aforementioned training, this paper adopts a cross-entropy loss $\mathscr{L}(\cdot)$. In summary, n-th devices local sQNN model $[\tilde{\boldsymbol{\theta}}^n; \tilde{\boldsymbol{\phi}}^n]$ is updated after L local iterations as:

$$\begin{bmatrix} \tilde{\boldsymbol{\theta}}_n \\ \tilde{\boldsymbol{\phi}}_n \end{bmatrix} \leftarrow \begin{bmatrix} \boldsymbol{\theta}_n \\ \boldsymbol{\phi}_n \end{bmatrix} - \eta_t \begin{bmatrix} \sum_{t=1}^{T_{Local}} \nabla_{\boldsymbol{\theta}_n^t} \mathscr{L}(\boldsymbol{\phi}_n, \boldsymbol{\theta}_n^t) \\ \sum_{t=1}^{T_{Local}} \nabla_{\boldsymbol{\phi}_n^t} \mathscr{L}(\boldsymbol{\phi}_n^t, \tilde{\boldsymbol{\theta}}_n) \end{bmatrix}, \tag{13}$$

where η_t and T_{Local} denote a learning rate at t and the number of local iterations, respectively.

By conducting pole-training in addition to conventional angle training, various channel conditions can be considered. When the channel conditions are good enough, it is possible to all gates and measurement parameters, which introduces best performance. However, on the other hand, if the channel conditions are poor, our proposed algorithm can deliver at least trained parameters in measurement. However, in conventional methods which has no training over measurement, there are no parameters to transmit. Therefore, conducting pole-training for parameter training in measurement is beneficial to take care of various channel conditions.

C. SUPERPOSITION CODING IN SATELLITE-GROUND CHANNEL

In each communication round, the n-th device uses the sQNN architecture to send either only its pole parameters $\tilde{\boldsymbol{\theta}}^n$, or both its pole and angle parameters $[\tilde{\boldsymbol{\theta}}^n; \tilde{\boldsymbol{\phi}}^n]$, depending on the communication channel conditions, energy availability, and other time-varying environmental factors. The ground local-QDL device n transmits a signal $\mathbf{x}_n$ to the server using the same radio resource block. This signal is given by,

$$\mathbf{x}_n = \sum_{i=1}^{2} \mathbf{s}_{n,i}, \tag{14}$$

where $\mathbf{s}_{n,i} \in \mathscr{S}_n$ is the i-th symbol for device n, and $\mathscr{S}_n$ is the Gaussian codebook for this device. The symbols are assumed to have zero mean and power P_i, for all $i \in \mathbb{N}[1, 2]$ and $n \in \mathbb{N}[1, N]$. Each local device encodes its raw data at a code rate of u.

Assuming that the user's location is stationary in the considered interval and considering both small-scale fading and large-scale fading, the channel model between local QDL device n and LEO satellite is expressed as,

$$g_n = \sqrt{G_s \cdot G_n (\frac{c}{4\pi f_c d_n})^2 \delta_n}, \tag{15}$$

where (G_s, G_n), d_n, δ_n c, and f_c are the antenna gains of satellite and local-QDL device n, the distance from the satellite to device n, Rayleigh fading, light speed, and center frequency, respectively.

D. AGGREGATION WITH SUCCESSIVE DECODING

The received signal sent by device n at the server, denoted by $\mathbf{y}_n$, is given by,

$$\mathbf{y}_n = \mathbf{g}_n^{\dagger} \mathbf{x}_n + \mathbf{n}_n = \mathbf{g}_n^{\dagger} \sum_{i=1}^{S} \mathbf{s}_{n,i} + \mathbf{n}_n, \tag{16}$$

where $\mathbf{n}_n \sim \mathscr{CN}(0, \sigma^2)$ represents the additive white Gaussian noise (AWGN). The signal-to-interference-noise ratio (SINR) for the i-th message which can be denoted as $s_{n,i}$ is given by

$$\gamma_{n,i} = \frac{P_i \cdot |\mathbf{g}_k^H \mathbf{s}_{n,i}|^2}{\sigma^2 + \sum_{i'=i+1}^{S} P_{i'} \cdot |\mathbf{g}_n^H \mathbf{s}_{n,i'}|^2}, \tag{17}$$

where

$$\sum_{i=1}^{I} P_i = P \tag{18}$$

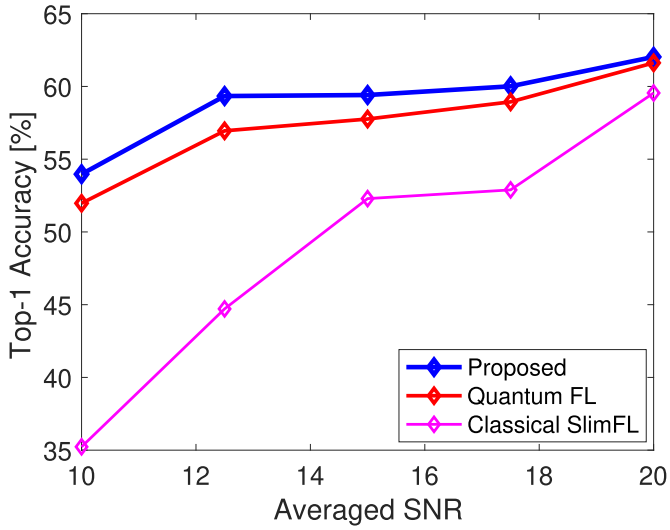

FIGURE 4. Averaged SNR *vs.* Top-1 Accuracy.

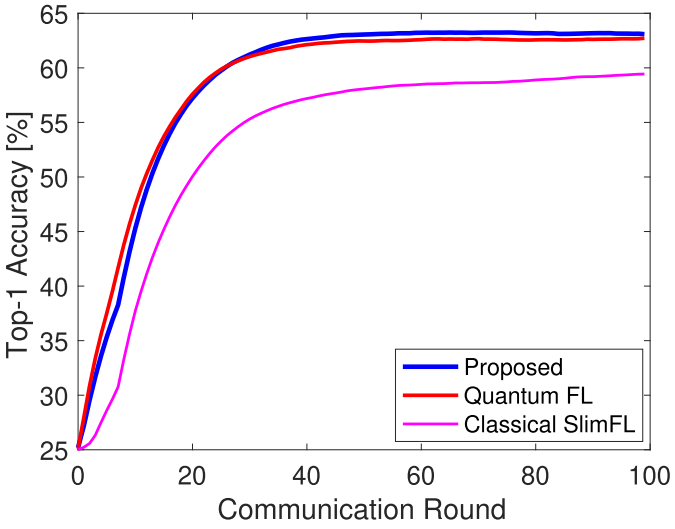

FIGURE 5. Learning curve $(\alpha, \bar{\gamma}) = (100, 20)$.

and σ^2 denotes the noise power. Using the Shannon capacity formula with a Gaussian codebook [42], the received throughput $R_{n,i}$ for the i-th symbol transmitted by device n with bandwidth W is given by,

$$R_{n,i} = W \log_2(1 + \gamma_{n,i}) \quad \text{(bits/sec)}. \tag{19}$$

If the transmitter encodes raw data at a code rate of u, the receiver can successfully decode the i-th encoded data if

$$(R_{n,i} \geq u) \wedge \ldots \wedge (R_{n,1} \geq u) := c_{n,i}, \tag{20}$$

and here, if $c_{n,i} = 1$, the i-th model configuration (e.g., $\boldsymbol{\phi}_n$ or $\boldsymbol{\theta}_n$) for device n will be included in the global model aggregation. The server aggregates the uploaded parameters and creates a global sQNN, represented by $[\tilde{\boldsymbol{\theta}}_0; \tilde{\boldsymbol{\phi}}_0]$, *i.e.*,

$$\begin{bmatrix} \tilde{\boldsymbol{\theta}}_0 \\ \tilde{\boldsymbol{\phi}}_0 \end{bmatrix} \leftarrow \begin{bmatrix} \frac{1}{\sum_{n=1}^{N} c_{n,1}} \sum_{n=1}^{N} c_{n,1} \tilde{\boldsymbol{\theta}}_n \\ \frac{1}{\sum_{n=1}^{N} c_{n,2}} \sum_{n=1}^{N} c_{n,2} \tilde{\boldsymbol{\phi}}_n \end{bmatrix}, \tag{21}$$

where indicator functions $c_{n,1}$ and $c_{n,2}$ keep track of the number of times the pole and angle parameters are uploaded, respectively. The devices then download the updated global sQNN $[\tilde{\boldsymbol{\theta}}_0; \tilde{\boldsymbol{\phi}}_0]$ and repeat the process until convergence is reached.

Note that the consideration of superposition coding and successive decoding in ground stations and satellites is not burden because the ground stations usually have no limitations in terms of communication systems design and

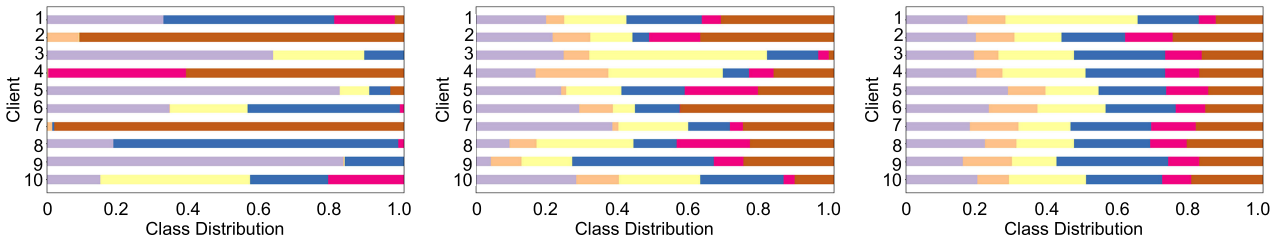

(a) Maximum non-iid ($\alpha = 0.1$). (b) Moderate non-iid ($\alpha = 1$). (c) Minimum non-iid ($\alpha = 10$).

FIGURE 6. Non-iidness where individual colors stand for distinct classes and the corresponding lengths represent the amount of data.

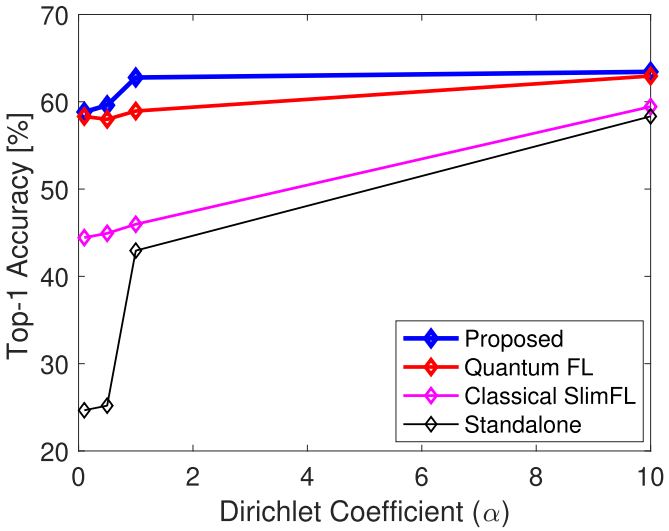

FIGURE 7. Non-IIDness *vs.* Top-1 Accuracy.

implementation. In satellites, the communication systems are not limited in terms of computational overhead. Usually in space communications, the performance itself is of our major interests.

IV. PERFORMANCE EVALUATION

A. SETUP

1) BENCHMARKS

The considered benchmark schemes have different average signal-to-noise ratios (SNRs), *i.e.*,

$$\bar{\gamma} = P/\sigma^2 \in \{10, 12.5, 15, 17.5, 20\}\,[\text{dB}]. \tag{22}$$

This paper also aims to investigate the effect of non-identically distributed data (non-IID) on SQFL by using a data-splitting method based on the Dirichlet coefficient α [43]. As benchmark schemes, two FL comparisons are designed as follows: *i)* "Classical SlimFL" with superposition coding and successive decoding [11] and *ii)* "Quantum FL" without these techniques to investigate the impact of communication opportunities.

2) ENVIRONMENT AND HYPERPARAMETER SETUP

All experiments were conducted using classical computers with NVIDIA RTX 2080Ti graphics processing units (GPUs). We use python v3.8.10, pytorch v1.12.1, CUDA v11.3, CUDNN v8, and torchquantum v0.1.2 [44]. The number of trainable parameters in sQNN is 82. Among them, the number of parameters in $\boldsymbol{\phi}$, and $\boldsymbol{\theta}$ is 80 and 2, respectively. The initial learning rate is 0.01, and the Adam optimizer trains sQNN. The parameters are adopted based on the realistic satellite-ground communications characteristics [40], *i.e.*, $f_c = 20\,\text{GHz}$, $W = 800\,\text{MHz}$, $h = 600\,\text{km}$, $P = 338\,\text{mW}$, $u = 8 \times 10^6\,\text{bit/s}$, $G_s = G_n = 2$, and $\forall \delta_n \sim \exp(1)$.

B. NUMERICAL RESULTS

1) IMPACT ON SNR

An experiment is conducted to investigate how the channel condition affects performance. Fig. 4 represents the relationship between the averaged SNR $\bar{\gamma}$, which is formulated in (17), and top-1 accuracy. According to [11], low SNR occurs as a divergence of classical SlimFL. When SNR is low, the top-1 accuracy records relatively low and vice versa. In addition, the convergence bound can be closed in high SNR conditions. Nevertheless, our SQFL framework performs better than QFL framework. The only difference is utilizing SC and SD which improves communication. In summary, these results corroborate that our SQFL framework shows

robustness to low SNR compared to QFL framework due to SC and SD.

2) IMPACT ON QUANTUM COMPUTING

To investigate the benefits of utilizing quantum computing, the ablation of quantum computing is conducted. Fig. 5 represents top-1 accuracy of SQFL, QFL, and Classical SlimFL with $\bar{\gamma} = 20$ and $\alpha = 100$, which can be regarded as perfect communication and ideal identical distribution (IID). SQFL and QFL show 3.65% and 3.22% higher performance than standard classical federated learning frameworks, respectively. According to [22], quantum computing can perform better than classical neural networks given the same number of parameters, which is a similar result.

3) ROBUSTNESS TO NON-IIDNESS

To investigate the impact of non-IID data distributions over ground devices, the experiments with various Dirichlet coefficient $\alpha = \{0.1, 1.0, 10\}$ are conducted, wherein higher α implies the distributions closer to IID. The corresponding distributions are simulated and visualized as presented in Fig. 6. Then, Fig. 7 represents the relationship between α and top-1 accuracy. As α gets smaller, the performance degradation is more severe. In addition, top-1 accuracy records the highest when $\alpha = 10$. Our framework shows the least performance degradation when the data distribution is non-IID. This verifies that our framework shows robustness to non-IIDness.

V. CONCLUDING REMARKS

This paper proposes a dynamic quantum federated learning framework for satellite-ground communication that utilizes slimmable quantum neural networks. By combining pole-to-angle training with joint superposition coding and successive decoding, our slimmable quantum federated learning approach demonstrates improved performance in both computing and communication. We also show that our SQFL framework is robust to low signal-to-noise ratios and non-IIDness. In future work, we plan to extend our approach to multi-LEO scenarios and investigate the optimal power allocation for superposition coding which is essential for next-generation 6G non-terrestrial networks.

REFERENCES

[1] *Low Earth Orbit (LEO) Satellites Global Market Report 2020–30: COVID-19 Growth and Change*, Business Research, London, U.K., 2021.

[2] A. Hills, J. M. Peha, J. Munk, and S. Pogorelc, "Controlling antenna sidelobe radiation to mitigate Ku-band LEO-to-GEO satellite interference," *IEEE Access*, vol. 11, pp. 71154–71163, 2023.

[3] L. Zhen, Y. Wang, K. Yu, G. Lu, Z. Mumtaz, and W. Wei, "Reliable uplink synchronization maintenance for satellite-ground integrated vehicular networks: A high-order statistics-based timing advance update approach," *IEEE Trans. Intell. Transp. Syst.*, vol. 24, no. 2, pp. 2097–2110, Feb. 2023.

[4] K. Kim, J.-H. Lee, S. Jung, J. Kim, and J.-H. Kim, "Stabilized detection accuracy maximization using adaptive SAR image processing in LEO networks," *IEEE Trans. Veh. Technol.*, vol. 71, no. 5, pp. 5661–5665, May 2022.

[5] Y. Wu, G. Hu, F. Jin, and J. Zu, "A satellite handover strategy based on the potential game in LEO satellite networks," *IEEE Access*, vol. 7, pp. 133641–133652, 2019.

[6] J. Tang, D. Bian, G. Li, J. Hu, and J. Cheng, "Resource allocation for LEO beam-hopping satellites in a spectrum sharing scenario," *IEEE Access*, vol. 9, pp. 56468–56478, 2021.

[7] Y. Hao, Z. Song, Z. Zheng, Q. Zhang, and Z. Miao, "Joint communication, computing, and caching resource allocation in LEO satellite MEC networks," *IEEE Access*, vol. 11, pp. 6708–6716, 2023.

[8] H. Chen, M. Xiao, and Z. Pang, "Satellite-based computing networks with federated learning," *IEEE Wireless Commun.*, vol. 29, no. 1, pp. 78–84, Feb. 2022.

[9] J. So, K. Hsieh, B. Arzani, S. Noghabi, S. Avestimehr, and R. Chandra, "FedSpace: An efficient federated learning framework at satellites and ground stations," 2022, *arXiv:2202.01267*.

[10] D. Kwon, J. Jeon, S. Park, J. Kim, and S. Cho, "Multiagent DDPG-based deep learning for smart ocean federated learning IoT networks," *IEEE Internet Things J.*, vol. 7, no. 10, pp. 9895–9903, Oct. 2020.

[11] W. J. Yun, Y. Kwak, H. Baek, S. Jung, M. Ji, M. Bennis, J. Park, and J. Kim, "SlimFL: Federated learning with superposition coding over slimmable neural networks," *IEEE/ACM Trans. Netw.*, early access, Jan. 2, 2023, doi: 10.1109/TNET.2022.3231864.

[12] H. Baek, W. J. Yun, Y. Kwak, S. Jung, M. Ji, M. Bennis, J. Park, and J. Kim, "Joint superposition coding and training for federated learning over multi-width neural networks," in *Proc. IEEE Conf. Comput. Commun. (INFOCOM)*, May 2022, pp. 1729–1738.

[13] Y. Kwak, W. J. Yun, J. P. Kim, H. Cho, J. Park, M. Choi, S. Jung, and J. Kim, "Quantum distributed deep learning architectures: Models, discussions, and applications," *ICT Exp.*, vol. 9, no. 3, pp. 486–491, Jun. 2023.

[14] M. Jaber, M. A. Imran, R. Tafazolli, and A. Tukmanov, "5G backhaul challenges and emerging research directions: A survey," *IEEE Access*, vol. 4, pp. 1743–1766, 2016.

[15] C. Zhang, H. Lu, and Z. Gu, "Analysis and optimization of cache-enabled mmWave HetNets with integrated access and backhaul," *IEEE Trans. Wireless Commun.*, vol. 22, no. 10, pp. 6993–7007, Oct. 2023.

[16] E. Farhi, J. Goldstone, and S. Gutmann, "A quantum approximate optimization algorithm," 2014, *arXiv:1411.4028*.

[17] F. Arute et al., "Quantum supremacy using a programmable superconducting processor," *Nature*, vol. 574, no. 7779, pp. 505–510, 2019.

[18] S. Lloyd, M. Mohseni, and P. Rebentrost, "Quantum algorithms for supervised and unsupervised machine learning," 2013, *arXiv:1307.0411*.

[19] J. Choi and J. Kim, "A tutorial on quantum approximate optimization algorithm (QAOA): Fundamentals and applications," in *Proc. Int. Conf. Inf. Commun. Technol. Converg. (ICTC)*, Oct. 2019, pp. 138–142.

[20] Y. Kwak, W. J. Yun, S. Jung, J.-K. Kim, and J. Kim, "Introduction to quantum reinforcement learning: Theory and PennyLane-based implementation," in *Proc. Int. Conf. Inf. Commun. Technol. Converg. (ICTC)*, Oct. 2021, pp. 416–420.

[21] C. Park, W. J. Yun, J. P. Kim, T. K. Rodrigues, S. Park, S. Jung, and J. Kim, "Quantum multi-agent actor-critic networks for cooperative mobile access in multi-UAV systems," *IEEE Internet Things J.*, early access, Jun. 5, 2023, doi: 10.1109/JIOT.2023.3282908.

[22] W. J. Yun, J. Park, and J. Kim, "Quantum multi-agent meta reinforcement learning," in *Proc. AAAI Conf. Artif. Intell.*, Washington, DC, USA, Feb. 2023, pp. 11087–11095.

[23] J. Choi, S. Oh, and J. Kim, "The useful quantum computing techniques for artificial intelligence engineers," in *Proc. Int. Conf. Inf. Netw. (ICOIN)*, Barcelona, Spain, Jan. 2020, pp. 1–3.

[24] W. J. Yun, J. P. Kim, S. Jung, J. Park, M. Bennis, and J. Kim, "Slimmable quantum federated learning," in *Proc. ICML Workshop Dyn. Neural Netw.*, Baltimore, MD, USA, Jul. 2022, pp. 1–5.

[25] J. Choi, S. Oh, and J. Kim, "A tutorial on quantum graph recurrent neural network (QGRNN)," in *Proc. Int. Conf. Inf. Netw. (ICOIN)*, Jan. 2021, pp. 46–49.

[26] T. V. K. Chaitanya and E. G. Larsson, "Bits-to-symbol mappings for superposition coding based HARQ systems," in *Proc. IEEE Wireless Commun. Netw. Conf. (WCNC)*, Apr. 2013, pp. 2468–2472.

[27] J.-H. Wui and D. Kim, "Cognitive relaying systems based on network and superposition coding in multiple access primary channels," in *Proc. IEEE Int. Conf. Signal Process., Commun. Comput. (ICSPCC)*, Sep. 2011, pp. 1–5.

[28] M. Sellathurai, P. Guinand, and J. Lodge, "Approaching near-capacity on a multi-antenna channel using successive decoding and interference cancellation receivers," *J. Commun. Netw.*, vol. 5, no. 2, pp. 116–123, Jun. 2003.
[29] R. M. Pujahari and A. Tanwar, "Quantum federated learning for wireless communications," in *Federated Learning for IoT Applications*. Springer, 2022, pp. 215–230.
[30] M. Chehimi and W. Saad, "Quantum federated learning with quantum data," in *Proc. IEEE Int. Conf. Acoust., Speech Signal Process. (ICASSP)*, May 2022, pp. 8617–8621.
[31] H. Wang, Z. Li, J. Gu, Y. Ding, D. Z. Pan, and S. Han, "QOC: Quantum on-chip training with parameter shift and gradient pruning," in *Proc. ACM/IEEE Design Autom. Conf. (DAC)*, San Francisco, CA, USA, Jul. 2022, pp. 655–660.
[32] S. Park, J. P. Kim, C. Park, S. Jung, and J. Kim, "Quantum multi-agent reinforcement learning for autonomous mobility cooperation," *IEEE Commun. Mag.*, early access, Aug. 28, 2023, doi: 10.1109/MCOM.020.2300199.
[33] H. Baek, S. Park, and J. Kim, "Logarithmic dimension reduction for quantum neural networks," in *Proc. ACM Conf. Inf. Knowl. Manage. (CIKM)*, Birmingham, U.K., Oct. 2023, pp. 3738–3742.
[34] G. S. Kim, J. Chung, and S. Park, "Realizing stabilized landing for computation-limited reusable rockets: A quantum reinforcement learning approach," *IEEE Trans. Veh. Technol.*, early access, 2024.
[35] M. C. Caro, H.-Y. Huang, M. Cerezo, K. Sharma, A. Sornborger, L. Cincio, and P. J. Coles, "Generalization in quantum machine learning from few training data," *Nature Commun.*, vol. 13, no. 1, p. 4919, Aug. 2022.
[36] H.-Y. Huang, M. Broughton, J. Cotler, S. Chen, J. Li, M. Mohseni, H. Neven, R. Babbush, R. Kueng, J. Preskill, and J. R. McClean, "Quantum advantage in learning from experiments," *Science*, vol. 376, no. 6598, pp. 1182–1186, Jun. 2022.
[37] J. Qi, C.-H.-H. Yang, P.-Y. Chen, and M.-H. Hsieh, "Theoretical error performance analysis for variational quantum circuit based functional regression," *npj Quantum Inf.*, vol. 9, no. 1, p. 4, Jan. 2023.
[38] M. Schuld and N. Killoran, "Quantum machine learning in feature Hilbert spaces," *Phys. Rev. Lett.*, vol. 122, no. 4, Feb. 2019, Art. no. 040504.
[39] M. Schuld and N. Killoran, "Is quantum advantage the right goal for quantum machine learning?" *PRX Quantum*, vol. 3, no. 3, Jul. 2022, Art. no. 030101.
[40] L. You, X. Qiang, C. G. Tsinos, F. Liu, W. Wang, X. Gao, and B. Ottersten, "Beam squint-aware integrated sensing and communications for hybrid massive MIMO LEO satellite systems," *IEEE J. Sel. Areas Commun.*, vol. 40, no. 10, pp. 2994–3009, Oct. 2022.
[41] N. Tripuraneni, B. Adlam, and J. Pennington, "Overparameterization improves robustness to covariate shift in high dimensions," in *Proc. NIPS*, vol. 34, 2021, pp. 13883–13897.
[42] C. E. Shannon, "A mathematical theory of communication," *Bell Syst. Tech. J.*, vol. 27, no. 3, pp. 379–423, Jul. 1948.
[43] T.-M. H. Hsu, H. Qi, and M. Brown, "Measuring the effects of non-identical data distribution for federated visual classification," 2019, *arXiv:1909.06335*.
[44] H. Wang, Y. Ding, J. Gu, Y. Lin, D. Z. Pan, F. T. Chong, and S. Han, "QuantumNAS: Noise-adaptive search for robust quantum circuits," in *Proc. IEEE Int. Symp. High-Perform. Comput. Archit. (HPCA)*, Los Alamitos, CA, USA, Apr. 2022, pp. 692–708.

SOOHYUN PARK received the B.S. degree in computer science and engineering from Chung-Ang University, Seoul, South Korea, in February 2019, and the Ph.D. degree in electrical and computer engineering, Korea University, Seoul, in August 2023.

She was a Postdoctoral Scholar with the Department of Electrical and Computer Engineering, Korea University, from September 2023 to February 2024. She has been an Assistant Professor with Sookmyung Women's University, Seoul, since March 2024. Her research interests include deep learning theory and network/mobility applications, quantum neural network (QNN) theory and applications, QNN software engineering and programming languages, and AI-based autonomous control for distributed computing systems. She was a recipient of the ICT Express Best Reviewer Award, in 2021; the IEEE Seoul Section Student Paper Contest Awards; and the IEEE Vehicular Technology Society (VTS) Seoul Chapter Awards.

SOYI JUNG (Member, IEEE) received the B.S., M.S., and Ph.D. degrees in electrical and computer engineering from Ajou University, Suwon, Republic of Korea, in 2013, 2015, and 2021, respectively.

She has been an Assistant Professor with the Department of Electrical of Computer Engineering, Ajou University, since September 2022. Before joining Ajou University, she was a Researcher with Korea Testing and Research (KTR) Institute, Gwacheon, Republic of Korea, from 2015 to 2016; a Research Professor with Korea University, Seoul, Republic of Korea, in 2021; an Assistant Professor with Hallym University, Chuncheon, Republic of Korea, from 2021 to 2022; and a Visiting Scholar with the Donald Bren School of Information and Computer Sciences, University of California, Irvine, CA, USA, from 2021 to 2022. Her current research interests include network optimization for autonomous vehicles communications, distributed system analysis, big-data processing platforms, and probabilistic access analysis. She was a recipient of the Best Paper Award by KICS, in 2015; the Young Women Researcher Award by WISET and KICS, in 2015; the Bronze Paper Award from IEEE Seoul Section Student Paper Contest, in 2018; the ICT Paper Contest Award by Electronic Times, in 2019; and the IEEE ICOIN Best Paper Award, in 2021.

JOONGHEON KIM (Senior Member, IEEE) received the B.S. and M.S. degrees in computer science and engineering from Korea University, Seoul, South Korea, in 2004 and 2006, respectively; and the Ph.D. degree in computer science from the University of Southern California (USC), Los Angeles, CA, USA, in 2014.

He has been with Korea University, since 2019, where he is currently an Associate Professor with the Department of Electrical and Computer Engineering and also an adjunct Professor with the Department of Communications Engineering (co-operated by Samsung Electronics) and the Department of Semiconductor Engineering (co-operated by SK Hynix). Before joining Korea University, he was a Research Engineer with LG Electronics, Seoul, from 2006 to 2009; a Systems Engineer with Intel Corporation Headquarter, Santa Clara, Silicon Valley, CA, USA, from 2013 to 2016; and an Assistant Professor of computer science and engineering with Chung-Ang University, Seoul, from 2016 to 2019. He serves as an Editor for IEEE TRANSACTIONS ON VEHICULAR TECHNOLOGY and IEEE INTERNET OF THINGS JOURNAL. He was a recipient of the Annenberg Graduate Fellowship with the Ph.D. admission from USC, in 2009; the Intel Corporation Next Generation and Standards (NGS) Division Recognition Award, in 2015; the IEEE SYSTEMS JOURNAL Best Paper Award, in 2020; the IEEE ComSoc Multimedia Communications Technical Committee (MMTC) Outstanding Young Researcher Award, in 2020; and the IEEE ComSoc MMTC Best Journal Paper Award, in 2021. He also received the IEEE ICOIN Best Paper Award, in 2021; the IEEE ICTC Best Paper Award, in 2022; and the IEEE Vehicular Technology Society (VTS) Seoul Chapter Awards.